ISSN 2176-5480

22nd International Congress of Mechanical Engineering (COBEM 2013)
November 3-7, 2013, Ribeirão Preto, SP, Brazil

EXPERIMENTAL STUDY ON DIFFERENT CONFIGURATIONS OF CAPACITIVE SENSORS FOR MEASURING THE VOLUMETRIC CONCENTRATION IN TWO-PHASE FLOWS

Emerson dos Reis
Diego da Silva Cunha
Federal Institute of Education, Science and Technology of São Paulo - IFSP, campus of São Joãoda Boa Vista, Acesso Dr. João Batista Merlin, S/N – Jd. Itália, São João da Boa Vista/SP, Postal Code 13872-551.
emersonr@ifsp.edu.br, diegoif1@hotmail.com

Abstract. *Two-phase flows occur in the presence of two immiscible components inside pipelines or process equipments. They are commonly found in the chemical, food, energy and oil industries. For them, among the instruments used to measure the volumetric fraction of one phase, there are capacitive probes consisting basically of two parts: a sensor with electrodes mounted around the tube with guards and shielding forming a capacitor, and a capacitance transducer circuit. Capacitive probes are robust, simple to handle, no special safety and care is required as for gamma or X-rays based instruments, and they are relatively inexpensive. However, there are several challenges that still require investments in research for becoming capacitive probes widely used in industry. One of them is related to the different geometric configurations feasible for the electrodes, being the main ones the helical, the double ring and the concave configurations. Each one should have its own characteristics in terms of sensitivity, immunity to effect of phase distribution, the linearity of response, etc. In this work, capacitive sensors with these configurations were designed and assembled by keeping some similarity among them. Then, they were tested in a static test rig with a transducer circuit. They were mounted in the horizontal position and rotated around the axial axis with different amounts of air and deionized water in the section, such as a stratified smooth air-water flow. The results showed the characteristics of each different geometric configuration and allowed to compare themselves, showing that the double ring is the best configuration for measuring the volumetric concentration of two-phase air-water flows.*

Keywords: *Two-phase Flow, Capacitance Probe, Capacitive Sensor, Volumetric Void Fraction, Holdup*

1. INTRODUCTION

The gas-liquid flows in pipelines are frequently present in many process of energy, chemical, food, and petroleum industries. When flowing together, the gas and the liquid can generate a number of different spatial arrangements into the pipeline called of flow patterns or flow regimes, which depend on volumetric flow rate of each component, physical properties of phases, geometry of the pipe and gravity (Taitel and Barnea, 1976). These flow regimes determine the overall performance of the process, and instrumentation dedicated to measure parameters of those flows, as the volumetric concentration, has importance on their study, evaluation and control.

In a horizontal pipeline with low or moderate flow velocities, forces due to the gravity separate the gas from the liquid. The gas tends to accumulate in the upper section and the liquid in the lower section of the pipe, generating a liquid layer. Such phenomenon is present in different flow regimes: stratified smooth, wavy and slug flow (Taitel and Barnea, 1976). This type of event has importance to this study as discussed ahead.

Different non-intrusive techniques for measuring the volumetric concentration in gas-liquid piping flows were already presented, which should be optical, X-ray, gamma ray, ultrasonic or capacitive (Keska and Fernando, 1992). The capacitive technique has some advantages since it is of low cost and robust, and the dielectric permittivity of gas is many times different from the liquid mainly when it is the water. This technique is based on measuring the capacitance due to the electric field formed between a source-sensing pair of electrodes, which is dependent of the effective dielectric permittivity of the medium around them including the two-phase flow. Capacitive systems for measuring the volumetric concentration in gas-liquid flows are, basically, composed of two parts as shown in Fig. 1: (1) a sensor that comprises a source-sensing pair of electrodes installed on the outer surface or the flush to the inner surface of the pipe, guard electrodes (not shown) used to avoid distortions of the electric field out of the sensing region, and a electromagnetic external shield (not shown) that avoids external interferences; and (2) a transducer circuit connected between the electrodes' terminals, which usually converts the equivalent capacitance to a DC voltage level.

In the equivalent electric circuit in Fig. 1 (b), C_w is the capacitance between the electrode and the interface between the fluid and the internal wall of the dielectric pipe, thus it occurs on both sides and is due to the dielectric material of the tube, C_s is the capacitance formed between the outer surface of the electrode and electromagnetic shield, and it is can include the capacitance due to connection cables, and the capacitance C_e due to the presence of fluids in the region of the electrodes. R_e is electrical resistance (or inverse of conductance) in parallel with C_e due will resistivity (inverse of conductivity) of the flowing fluids.

ISSN 2176-5480

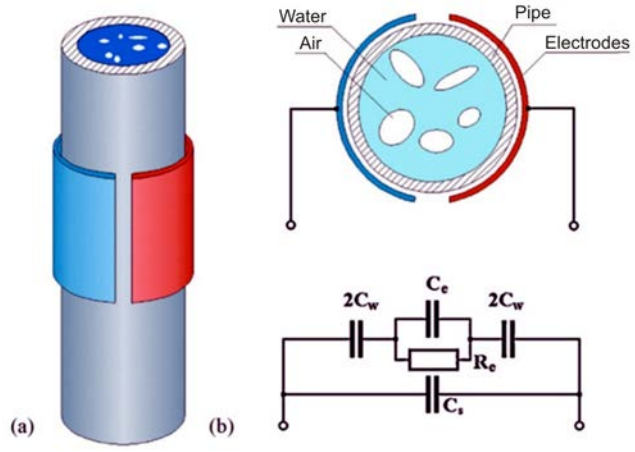

Figure 1. Capacitive sensor with external concave electrodes (a), equivalent electric circuit (b).

Different configurations of capacitive sensors' electrodes are possible (Sami *et al.*, 1980, Stott *et al.*, 1985, Kendoush and Sarkis, 1995), as in Fig. 2: parallel plates (a), concave plates (b), double ring (c), unidirectional (d), and double helix (e), having each one its own characteristics. The configurations (b), (c) and (e) are the most used in practical situations and, in a general way, concave electrodes are more sensitive and shows the most linear response, however, it is highly dependent on the spatial distribution of phases into the sensor, double ring has greater immunity to the distribution of the phases, however, it has low sensitivity and linearity of response, and the double helix has intermediate characteristics. Therefore, the geometric configuration of the electrodes determines the performance of the whole measurement system and, consequently, it is the key for use this technique in multiphase flows. The design of the electrodes' must be focused in the flow regimes to be monitored and in the quantity of interest that can be volumetric such as the holdup of gas or liquid, or linear such as the liquid layer thickness.

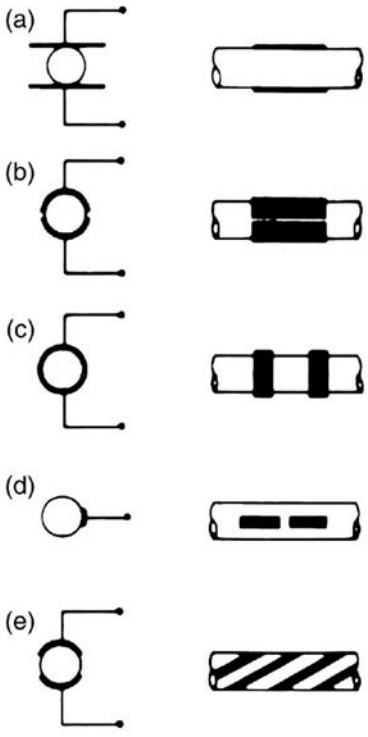

Figure 2. Electrodes' configurations: parallel plates (a), concave plates (b), double ring (c), unidirectional (d), double helix (e) (Kendoush and Sarkis, 1995).

Hence, through this paper, we provided additional information about the characteristics of three different geometric configurations of electrodes of a capacitive sensor: helical, concave and double ring electrodes, for applications on

ISSN 2176-5480

volumetric concentration in gas-liquid flows. All the studies were performed with water and air by using a bench for static tests.

2. EXPERIMENTAL APPARATUS

It was composed of a bench for static tests, three capacitive sensors with different geometric configurations of the electrodes, a capacitance transducer developed by dos Reis (2003) and a number of auxiliary equipments.

2.1 Bench for static tests

The bench for static tests was used to perform tests on each capacitive sensor is shown in Fig. 4. It is composed of a horizontal Plexiglas of about D = 34 mm ID pipe section with 3 mm of wall thickness, plugged in both extremities, and divided into two parts: a rotating test section, with an angle indicator, and a static section, with a micrometer and two liquid taps on the bottom of the tube. A nylon joint with o-rings allowed a rotating movement between the sections. The base had four screws that permitted adjusting its horizontal level. The micrometer, with a range from 25 to 50 mm, and a minor scale division equal to 0.01 mm, was used to adjust and measure the liquid layer thickness. There was a small hole called of gas tap in the figure which allowed the air to enter/exit from the pipe according to the liquid level under test. Two PVC joints were used to install and set the capacitive sensors (test section) to the bench.

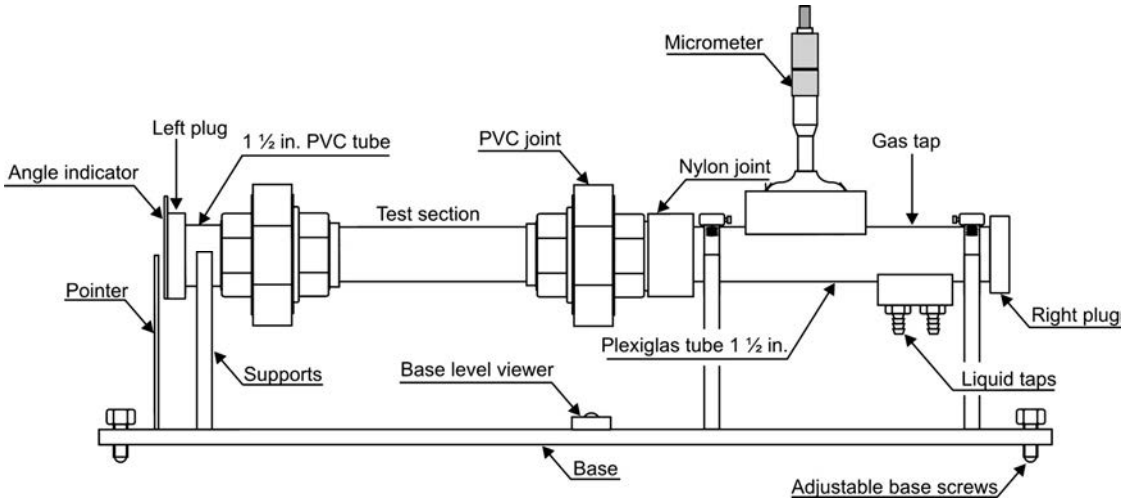

Figure 3. Schematic of the bench for static tests (dos Reis and Goldstein Jr., 2005a).

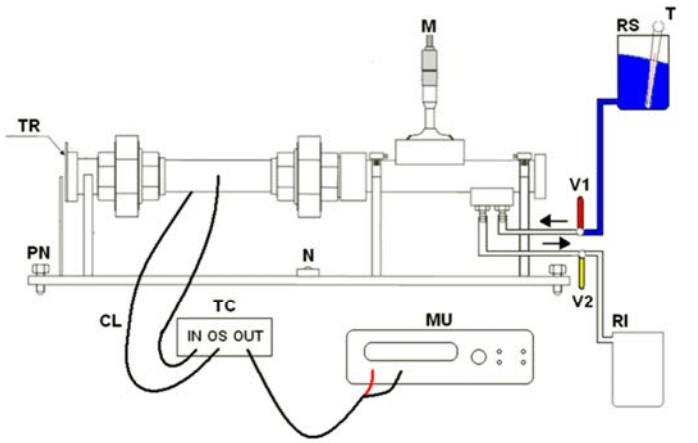

Figure 4. Experimental apparatus.

ISSN 2176-5480

According to the Fig. 4, during operation, water is injected from RS through V1 or removed to RI through V2. In this work, the water used for the tests was deionized, which avoided interference of the resistive component R_e in Fig. 1 (b) on the performance of the capacitance transducer circuit TC, connected to the capacitive sensor through the coaxial cables CL. The voltage level was measured by a voltmeter MU of 4 4/3 digits.

Preliminary tests with a fixed volume of water into the pipe which set the liquid layer thickness to be about h_L = 17 mm or $h_L/D \cong 0.50$, and with different values of the turning angle allowed perform evaluation on deviations due to eccentricities in the PVC joints, in the pipe and in the left plug (see Fig. 3). It was about +0.98 mm in the worst case from the minimal to the maximal measured value, representing a deviation of 0.03577 or 3.6% on the measure of the volumetric concentration of water.

2.2 Capacitive sensors

Three different geometrical configurations were tested: helical, concave and double ring. Figures 5 to 7 show the main dimension of each sensor. They were designed by keeping some proportion: all the electrodes had almost the same single area, and they were assembled on a section of about 300 mm of the same Plexiglas pipe with 33.85 mm of internal and 40.20 mm of external diameter, determined from four measurements performed around the perimeter.

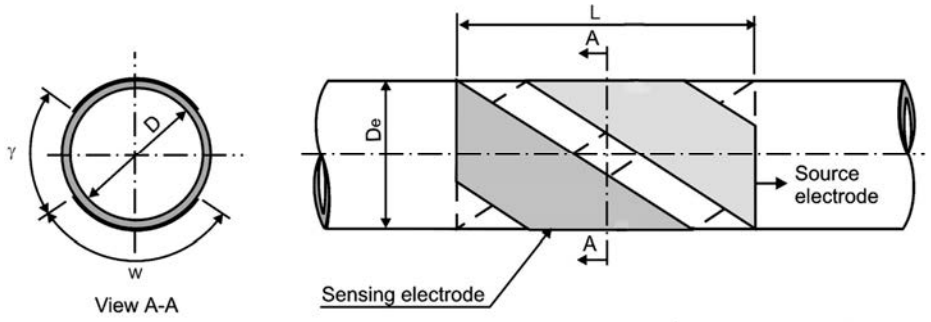

Figure 5. Helical electrodes' sensor

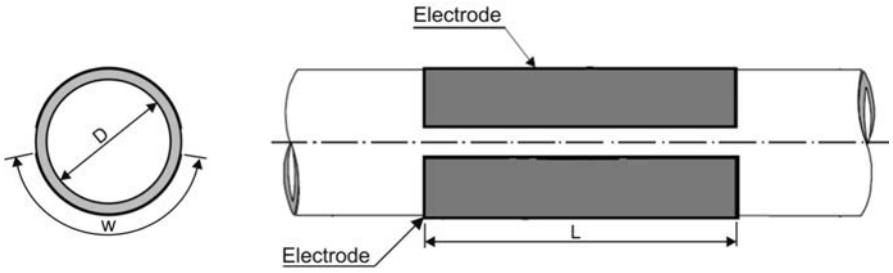

Figure 6. Concave electrodes' sensor.

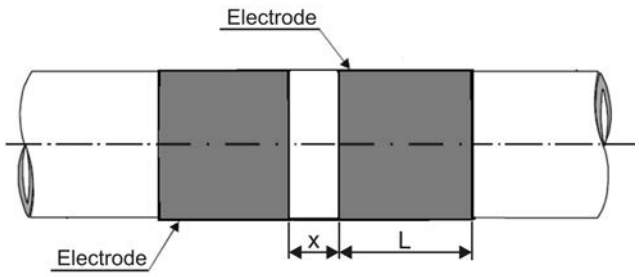

Figure 7. Double ring sensor.

Table 1 shows the dimensions of the electrodes of each sensor presented in Figs. 5 to 7 with D_e = 40.2 mm. The torsion angle of the helical sensor was 45°. The area of a single electrode was 0.005950, 0.005978 and 0.005935 m^2 for helical concave and double ring sensors, respectively. Therefore, it was almost the same among all three sensors.

ISSN 2176-5480

Table 1. Dimensions of the capacitive sensors.

Sensor	***L [mm]***	***w [mm]***	***x [mm]***	***[º]***
Helical	105.2	42.5	-	21.2
Concave	98.0	61.0	-	102.8
Double ring	47.0	$.D_e$	11.0	-

Figure 8 shows the capacitive sensors. One can see the electromagnetic shield of aluminum, the PVC joints in each side of the sensors and the BNC connectors. The electrodes were made of cupper sheet of 0.1 mm tick.

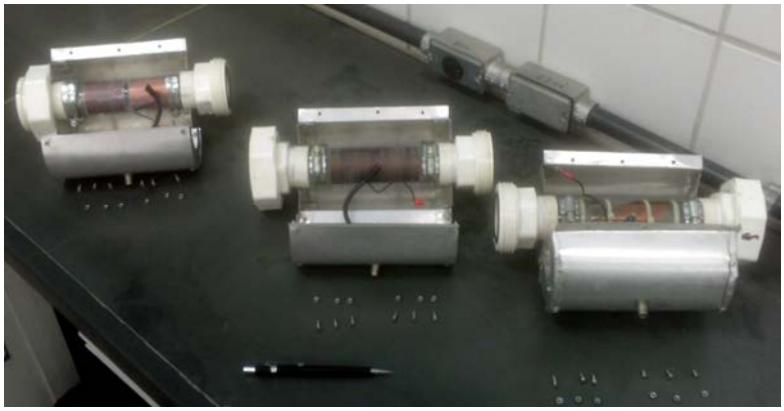

Figure 8. Double ring, concave and helical sensors from left to right.

2.3 Capacitance transducer

The capacitance transducer was based on the AC method as discussed by Mariolli *et al.* (1993), however, without the feedback circuitry. It was developed and assembled by dos Reis (2003) in his doctoral research.

In this work, it was calibrated using a bench of NPO 1% ceramic capacitors previously calibrated by dos Reis (2003) with a Hewlett Packard model HP 4284A LCR meter in the same excitation frequency of 1 MHz. The measurement uncertainty was ±0.0203 pF @ 95% of confidence interval. In addition, the warm up time was determined starting at t = 0 h the cold transducer connected to a 2.2 pF capacitor, and observing the output voltage variation. It was about 2 hours with ambient temperature of 26 ^{o}C. Figure 8 (a) shows the calibration curve, while (b) shows the warm up curve.

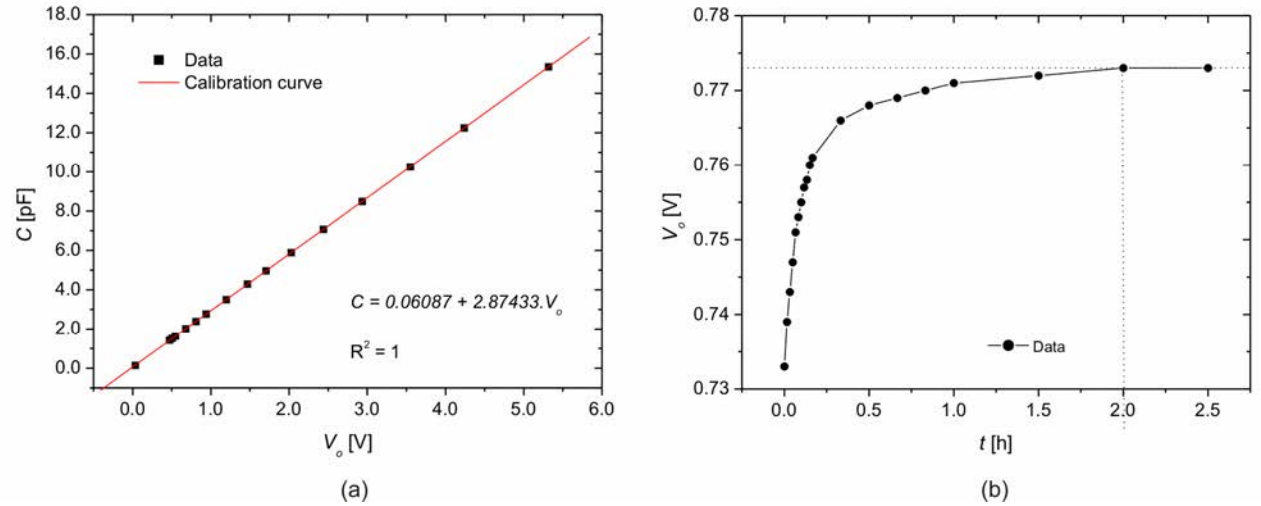

Figure 9. Calibration curve (a), warm up curve (b).

3. PRECEDURES AND DATA REDUCTION

The apparatus of Fig. 3 allowed generating a spatial arrangement of the water and air similar to the stratified smooth flow regime. It was considered the most suitable regime for evaluating the effect of the spatial arrangement on the sensors' performance, since it is the worst case when liquid and the gas are completely segregated.

ISSN 2176-5480

The experimental procedure concerned to register values of the transducer output voltage V_o for different liquid layer thickness h_L/D = 0.00 (pipe full filled of air), 0.19, 0.28, 0.37, 0.45, 0.54, 0.63, 0.72 and 1.00 (pipe full filled of water) in different angular positions of the sensors from the reference positions shown in Fig. 10 for each tested sensor, = -90.0°, -65.7°, -45.0°, -22.5°, 0.0°, +22.5°, +45.0°, +65.7° and +90.0° equal a ½ turn, which was sufficient to perform a complete evaluation of each sensor due to the symmetry in relation to the vertical plane passing through the center of the section. In Fig. 10 (a) and (b), the edge of the sensing electrode (showed in the figure) was in the bottom with = 0°. The source electrode was connected to an oscillating circuit which provided excitation sinusoidal signal. One will observe that there were differences of the sensor's sensitivity at near to the source and sensing electrodes, as discussed by Xie *et al.* (1990). Therefore, 72 data points were registered for each of the three sensors studied.

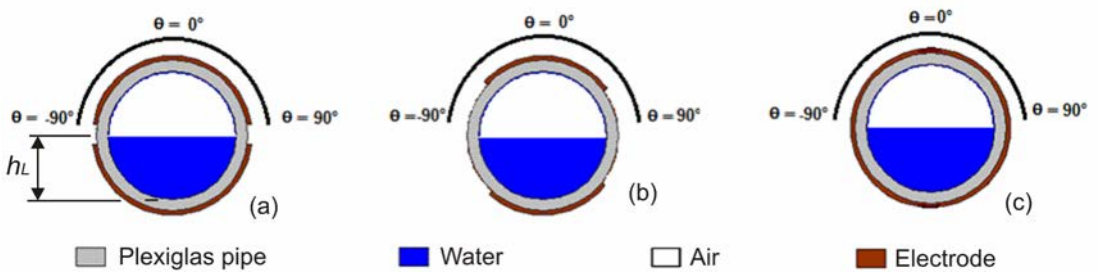

Figure 10. Reference positions of each capacitive sensor: concave (a), helical (b), double ring (c).

Data reduction was performed first converting the h_L/D in the volumetric concentration of liquid or hold up of liquid through Eq. (1). After that, the capacitances C were calculated from V_o by using the transducer's calibration curve. Following, the values of the non-dimensional capacitance C_n were calculated with Eq. (2), where C_{min} and C_{max} were the minimum and the maximum value of C with = 0 and = 1, respectively. It was done due to differences observed among the capacitance ranges, which were related to the geometrical characteristics of each sensor. Therefore, their responses could be compared through C_n.

$$= 1 - \frac{1}{\left\{ - a\cos\left[1 - 2\frac{h_L}{D}\right] + \left(1 - 2\frac{h_L}{D}\right)\sqrt{1 - \left(1 - 2\frac{h_L}{D}\right)^2}\right\}} \quad (1)$$

$$C_n = \frac{C - C_{\min}}{C_{\max} - C_{\min}} \quad (2)$$

Graphs of C_n versus for different values of , and of C_n versus for different values of were obtained. For these last ones, the data were fitted by the mathematical model represented by Eq. (3), where A_1 represented the mean value of C_n, A_2 the amplitude of the cosine function around the mean value, is the phase angle, is an additional degree of freedom and is the conversion factor from degrees to radians equal to /180 as needed by the curve fitting software. Mainly the values of A_1 and A_2 allowed evaluating the influence of the gas-liquid distribution on the performance of the capacitive sensors, as discussed ahead.

$$C_n = A_1 + A_2 \cos\left[.\left(- + \right)\right] \quad (3)$$

4. RESULTS ANS ANALYSIS

Table 2 presents the values of C_{min} and C_{max} for different and for each sensor tested. During the tests, the water temperature ranged from 24 to 28 °C, which could cause less than 1% of variation on the capacitance C of the sensors (dos Reis and Goldstein, 2005b).

Although the presented values of were calculated from the nominal values of h_L/D, given in the item 3 in Eq. (1), among all tests, a maximum deviation of only -3.0 % was observed between the nominal and the measured h_L/D. In Table 2, the percentile difference $\Delta C = 100.(C_{max} - C_{min})/C_m$, where C_m is the mean value from C_{max} to C_{min}. As can be observed, the capacitance for helical sensor ranged from 2.17 to 11.56 pF, from 6.02 to 18.34 pF for concave and from 1.66 to 9.21 for double ring. Therefore, the range was 9.39, 12.32 and 7.55 pF, respectively. The concave sensor presented the highest sensitivity and the double ring the lowest one, however, when referring to ΔC among all , the concave was the most affected sensor by the air-water distribution, with ΔC as higher as 62.8 % for equal to 0.43,

ISSN 2176-5480

while the double ring was the fewest affected sensor with ΔC lower than 3.6 % for equal to 0.0, which was only due to common voltage fluctuations observed in the transducer output. The helical sensor presented values of C_{min} and C_{max} near to the double ring, although its geometrical shape appeared to be conceived as mix between the concave and the double ring sensors, in relation to the range of measured capacitances, it is nearest to the double ring.

Table 2. Capacitance: minimal C_{min}, maximal C_{max}, and percentile differences ΔC for various .

	Helical			Concave			Double Ring		
[m^3/m^3]	C_{min} [pF]	C_{max} [pF]	ΔC [%]	C_{min} [pF]	C_{max} [pF]	ΔC [%]	C_{min} [pF]	C_{max} [pF]	ΔC [%]
0.000	2.17	2.23	2.7	6.02	6.06	0.7	1.66	1.72	3.6
0.126	3.38	4.2	21.6	6.04	10.2	51.2	3.46	3.57	3.1
0.232	4.1	4.99	19.6	6.09	11.02	57.6	4.17	4.3	3.1
0.324	4.92	5.79	16.2	6.21	11.82	62.2	4.88	5	2.4
0.430	5.82	6.59	12.4	6.53	12.51	62.8	5.53	5.67	2.5
0.554	6.77	7.42	9.2	9.07	13.51	39.3	6.1	6.22	1.9
0.686	8.13	8.6	5.6	11.7	14.46	21.1	6.76	6.88	1.8
0.773	8.99	9.38	4.2	13.63	15.35	11.9	7.38	7.49	1.5
1.00	11.53	11.56	0.3	18.31	18.34	0.2	9.20	9.21	0.1

Table 3 presents the fitting coefficients of Eq. (3) while Figs 11 to 13 show graphs of C_n *versus* for different values of in (a), and of C_n versus for different values of in (b). Some coefficients were not calculated if the sensor response is almost constant for different turning angles , as can be seen in Fig. Fig. 11 (b), 12 (b) and 13 (b) for = 0.0 (pipe full filled of air), = 1.0 (pipe full filled of water) and all them for the double ring sensor, which was minimally affected by the spatial arrangement of the air-water phases as discussed before on data of Table 2, therefore, only the A_1 representing the mean value of C_n was calculated.

Table 3. Fitting coefficients of Eq. (3) for helical, concave and double ring sensors.

	Helical				Concave				Double ring
[m^3/m^3]	A_1 [1]	A_2 [1]	$^{-1}$ [1]	[^{o}]	A_1 [1]	A_2 [1]	$^{-1}$ [1]	[^{o}]	A_1 [1]
0.000	0.002444	-	-	-	0.0004444	-	-	-	0.007111
0.126	0.17320	0.04412	1.8088	27.2	0.14967	0.16942	2.3239	-9.3	0.24389
0.232	0.25358	0.04761	1.7852	29.0	0.21346	0.21252	1.9976	-4.2	0.33989
0.324	0.3387	0.04761	1.8316	32.6	0.21224	0.26753	1.5163	-6.0	0.43311
0.430	0.42967	0.04195	1.7319	40.7	0.03206	0.49958	0.9651	3.0	0.51967
0.554	0.52479	0.03583	1.6404	34.0	0.3739	0.23925	1.3147	-0.5	0.59389
0.686	0.65795	0.02781	1.3228	37.1	0.58133	0.11249	1.9417	9.5	0.68089
0.773	0.74385	0.02618	1.0380	41.1	0.68503	0.07039	1.6529	21.3	0.76538
1.00	0.99933	-	-	-	0.99889	-	-	-	0.99967

Figures 11 (a), 12 (a) and 13 (a) correspond to the response of each tested sensor to different volumetric concentrations of liquid. Among all turning angles, the concave sensor presented the most scattered data points, meaning that it is highly affected by the water and air distribution. However, considering that linearity is always a desired characteristic for instruments, depending on the turning angle (= $\pm 45^o$ when the electrodes are positioned vertically), it becomes more linear (dos Reis and Goldstein Jr., 2005a). In Fig. 11 (a) for the helical sensor, the data points are less scattered than those of the concave one, being them more distant themselves within a variation of C_n about 0.1 in from 0.1 to 0.4, showing some influence of the water and air distribution. For the helical sensor, the data points indicate a "S" shaped curve of C_n *versus* , and the highest linearity is observed with = + 90^o when the edge of the source-sensing pair of electrodes, as seen in Fig. 10, is positioned vertically. In Fig. 13 (a) for the double ring sensor, the data points indicate to the same "S" shaped curve of C_n *versus* , similar to helical on the worst case of linearity when = $\pm 45^o$, however, the data points are very close themselves among different , therefore, showing a minimal influence of the water and air distribution on its performance. In the Figs. 11 (a), 12 (a) and 13 (a), the dashed straight lines are parallel to the line from (= 0; C_n = 0) to (= 1; C_n = 1), and they indicate regions within the data points were scattered, with deviations of C_n about 0.6 for concave and about 0.2 for helical and double ring sensors.

ISSN 2176-5480

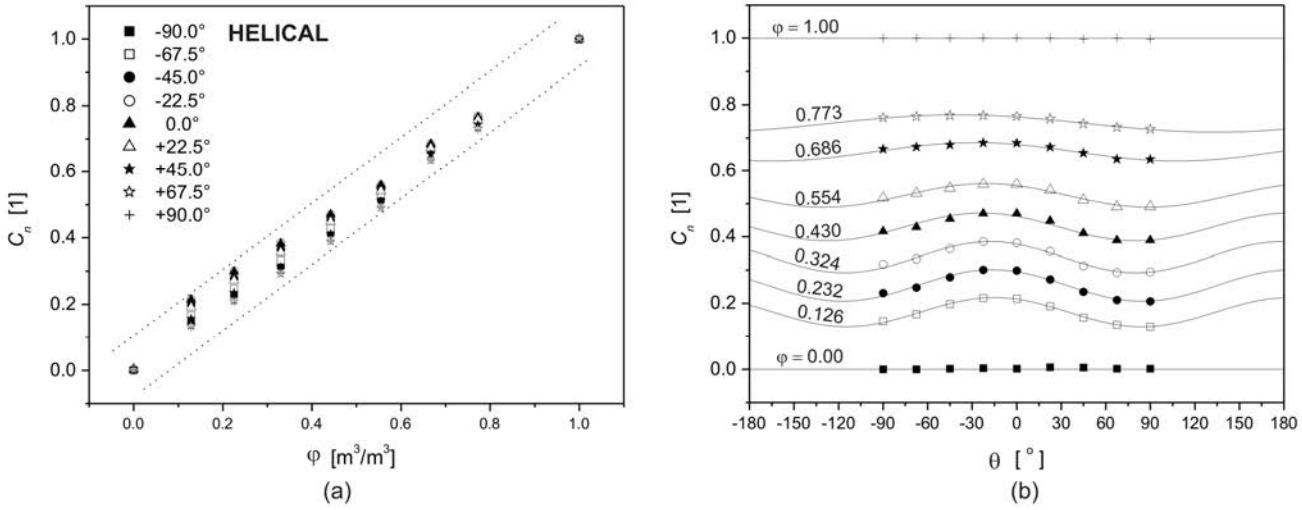

Figure 11. C_n for the helical electrodes' *versus* (a), and *versus* the turning angle with the fitting curves (b).

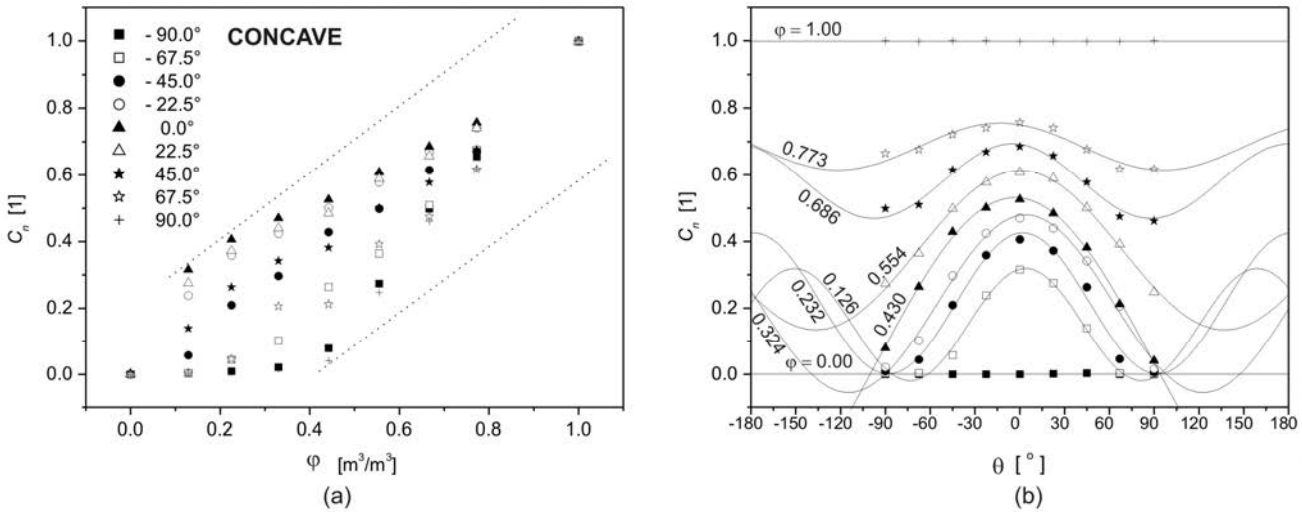

Figure 12. C_n for the concave electrodes' *versus* (a), and *versus* the turning angle with the fitting curves (b).

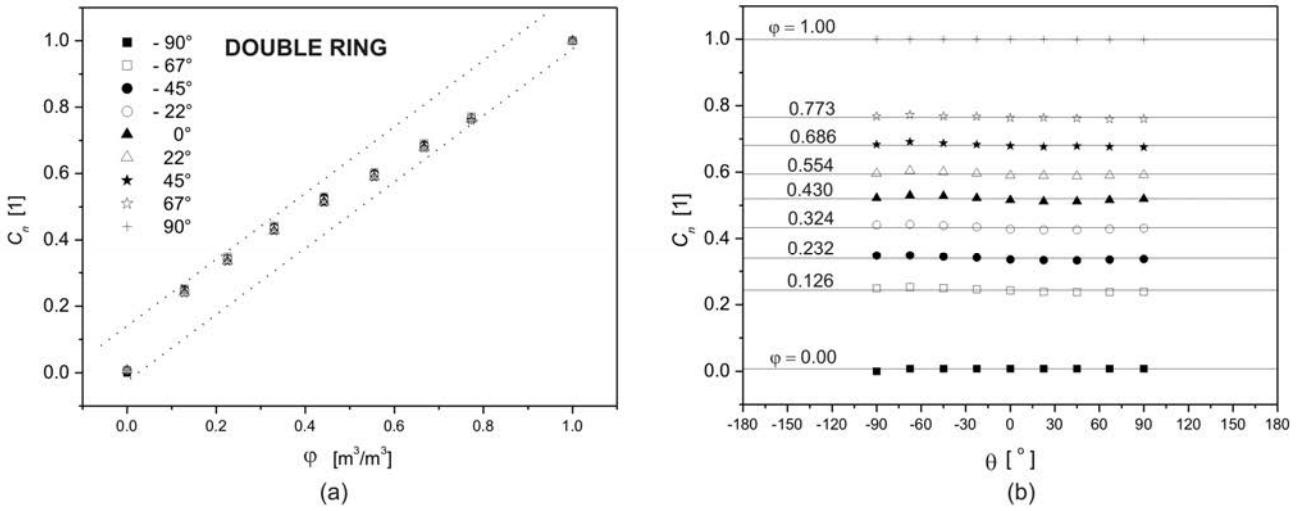

Figure 13. C_n for the double ring sensor *versus* (a), and *versus* the turning angle with the mean lines (b).

ISSN 2176-5480

Figures 11 (b), 12 (b) and 13 (b) show graphs of C_n *versus* the turning angle and with the fitting curves. The fitting coefficients of Eq. (3) are presented in the Table 3. A_1 represents the mean value of C_n, A_2 is the peak amplitude the variation of C_n around the mean value of a cosine function of , can be interpreted as the phase angle related to the departure of on the maximum of C_n from origin of the horizontal axis, and $^{-1}$ determines the number of "cycles" of the cosinusoidal function of C_n in each turn of the sensor given by .

One can observe in Fig. 11 (b) and in Table 3, A_1 increases while A_2, and $^{-1}$ decrease with for the helical sensor. Due to differences on the proximity of the bulk of water around the source-sensing pair of the helical electrodes from $= 0^o$, indicates that as high as the volumetric concentration as near the maximum of C_n to the origin of the axis , since the area near to the water of the sensing electrodes becomes higher by increasing . In relation to $^{-1}$, it indicates that, C_n gives two cycles at each turn of the sensor section, since $^{-1}$ is about 2 with lower . Heterogeneous distribution of the sensitivity in relation to the source and the sensor electrodes can diverge the C_n curves from the ideal cosinusoidal type behavior from the mathematical model represented by Eq. (3), consequently, it can also cause differences on calculated values of $^{-1}$.

Differently, the concave sensor A_1 doesn't only increases univocally with , while A_2 increases from $= 0$ to about 0.43 and decreases again until $= 1$. Values of about 0^o indicate that the maximum value of C_n occurred on $= 0^o$ with the electrodes on the horizontal position with the sensing one on the bottom surface as in Fig. 10 (a). Values of $^{-1}$ also about 2.0 also indicate that C_n gives two cycles at each turn of the sensor section.

Figure 13 (b) shows, again, that the C_n of the double ring sensor was minimally affected by the air water distribution.

5. CONCLUSIONS AND REMARKS

In this work, capacitive sensors with helical concave and double ring configurations were designed and assembled by keeping some similarity among them. They were tested in a bench for static tests with a transducer circuit, where they were mounted in the horizontal position and rotated around the axial axis with different amounts of air and deionized water in the section, such as a stratified smooth air-water flow, considered the most suitable regime for evaluating the effect of the spatial arrangement on the sensors' performance, since it is the worst case when liquid and the gas are completely segregated.

The results showed that the concave sensor presented the highest sensitivity and the double ring the lowest one, however, the concave was the most affected sensor by the air-water distribution while the double ring was the fewest affected sensor. The concave sensor also presented the highest linear response, however, it happened only with for a specific $= \pm 90^o$ and, small differences of from it can cause the response to become highly non-linear. Both helical and double ring presented similar non-linear responses, being the double ring minimally affected by the air-water distribution.

In addition, the helical sensor presented the characteristics similar to the double ring one, although its geometrical shape appeared to be conceived as mix between the concave and the double ring sensors. However, the double ring was the geometrical configuration less affected by the air-water distribution in relation the sensor's electrodes. Therefore, it was evaluated as the most suitable geometrical configuration for measuring the volumetric concentration in two-phase gas-liquid flows.

6. ACKNOWLEDGEMENTS

The support of FAPESP — Fundação de Amparo à Pesquisa do Estado de São Paulo, Brazil — is deeply appreciated.

7. REFERENCES

dos Reis, E., 2003, "*Study of pressure drop and phases distribution of the horizontal air–water slug flow in pipelines with "T" branch arms*". Ph.D. Thesis, College of Mechanical Engineering, UNICAMP (in Portuguese).

dos Reis, E., Goldstein Jr., L., 2005a, "A non-intrusive probe for bubble profile and velocity measurement in horizontal slug flows", Flow Measurement and Instrumentation, v. 16, n. 4, pp. 229-239.

dos Reis, E.; Goldstein Jr., L.2005b, "A procedure for correcting for the effect of fluid flow temperature variation on the response of capacitive void fraction meters". *Flow Measurement and Instrumentation*, v. 16, n. 3, p. 229.

Kendoush, A. A., Sarkis, Z. A., 1995, "Improving the accuracy of capacitance method for void fraction measurements". Experimental Thermal and Fluid Science, v. 11, n. 4, pp. 321-326.

Keska, J. K., Fernando, R. D., 1992, "An experimental study of liquid film thickness measurement in a two-phase flow". AICHE Symposium Series, Heat Transfer, San Diego.

Mariolli, D., Sardini, E., Taroni, A., 1993, "High-accuracy measurement techniques for capacitance transducers". *Measurement Science and Technology*, v. 4 ,n. 3, p. 337-343.

Sami. M., Abouelwafa A., Kendall, J. M., 1980. "The use of capacitance for phase percentage determination in multiphase pipelines". *IEEE Trans. on Measurement and Instrumentation*, v. IM-29, n. 1, p. 24-27.

Stott, A. L., Green, R. G., Seraji, K., 1985, "Comparison of the use of internal and external electrodes for the measurement of the capacitance and conductance of fluids in pipes". *Journal of Physics E - Scientific Instruments*, v. 18, n. 7, p. 587-592.

Taitel, Y., Dukler, A. E., 1976, "A model for predicting flow regime transitions in horizontal and near horizontal gas-liquid flow". AIChE Journal, v. 22, n. 1, pp. 47-55.

Xie, C. G., Stott, A. L., Plaskowski, A., Beck, M. S., 1990, "Design of capacitance electrodes for concentration measurement of two-phase flow". Measurement Science and Technology, v. 1, n. 65, pp. 65-78.

8. RESPONSIBILITY NOTICE

The authors are the only responsible for the printed material included in this paper.